MODEL UNCERTAINTIES IN NLFEAS OF RC SYSTEMS UNDER CYCLIC LOADS

Available online at www.easdprocedia.org
EASD Procedia EURODYN (2020) 3527-3547

EASD Procedia

EURODYN 2020
XI International Conference on Structural Dynamics
M. Papadrakakis, M. Fragiadakis, C. Papadimitriou (eds.)
Athens, Greece, 23–26 November 2020

MODEL UNCERTAINTIES IN NLFEAs OF RC SYSTEMS UNDER CYCLIC LOADS

Paolo Castaldo[1], Diego Gino[1], Guglielmo Amendola[1]and Elena Miceli[1]

[1] Politecnico di Torino
Corso Duca degli Abruzzi 24, Turin, Italy
e-mail: {paolo.castaldo@polito.it, diego.gino@polito.it, guglielmo.amendola@polito.it, elena.miceli@studenti.polito.it}

Keywords: NLFEAs; model uncertainties; reinforced concrete structures; cyclic loads

Abstract. *This work is focused on the resistance model uncertainties in non-linear finite element analyses (NLFEAs) for reinforced concrete structures under cyclic loading conditions. In detail, different walls experimentally tested are numerically reproduced by means of appropriate plane stress finite elements (FE) structural models within different assumptions and numerical codes. After that, the values of the global resistances computed through numerical simulations are compared to the experimental outcomes to evaluate the influence of the different assumptions on the mechanical behaviour of reinforced concrete members subjected to cyclic loads.*

ISSN:2311-9020
Peer-review under responsibility of the Organizing Committee of EURODYN 2020.
doi: 10.47964/1120.9289.20047

1 INTRODUCTION

The adoption of non-linear finite element analyses (NLFEAs) for structural design and assessment of structures and infrastructures is one of the main innovation in civil engineering in the last decades. Such kind of instruments are able to reproduce with accuracy the mechanical behaviour of reinforced concrete (RC) structures. In order to allow the correct use of NLFEAs from designers and analysts, several guidelines and recommendations for NLFEAs have been developed [1]-[2] to assess the safety and resilience of infrastructure systems [3]-[4]. Moreover, several applications are reported in the literature with examples of appropriate procedures devoted to calibrate and interpret the outcomes from NLFE models [5]-[6]. Over the years, different methodologies denoted as "safety formats" for NLFEAs have been proposed by several researchers [7]-[8] and international codes [9]-[10] as well as their applications have been discussed by [11]-[13]. In the mentioned above methods, the aleatory uncertainties associated to material properties and the epistemic uncertainties related to the numerical definition of the structural model need to be properly treated in order to derive reliability-based values of the global structural responses [14]-[18]. Concerning the materials uncertainty, the corresponding variability is well known and reported in the scientific literature, whereas the resistance model uncertainty associated with NLFEAs needs to be investigated due to the possible different modelling hypotheses that can be assumed by engineers and analysts to model some physical phenomena without a perfect knowledge. For this reason and especially within seismic field, an appropriate evaluation of the resistance model uncertainties for NLFEAs of RC structures is still necessary with the aim to account for their influence in presence of cyclic loads. In detail, different assumptions can be performed regarding the parameters that govern the equilibrium, kinematic compatibility and constitutive equations in cyclic loading configurations according to scientific literature and numerical codes. In the present study, the cyclic responses of ten experimental tests on shear walls known from the literature [19]-[21] are compared to the related numerical outcomes derived from appropriate 2D NLFEAs. In detail, a multitude of NLFEAs are developed for each experimental test in order to investigate the effect of each assumption on the global resistance of each structural element. This comparison is herein based on the definition of different eighteen plausible structural models combing different types of numerical code with different mechanical constitutive laws for the reinforced concrete elements in cyclic loading configurations.

2 UNCERTAINTIES WITHIN SAFETY FORMATS FOR NLFEAS

Commonly, both epistemic and aleatory uncertainties influence structural engineering problems [14]. Focusing on the epistemic uncertainties, all the choices performed to define a specific numerical model (i.e., modelling hypotheses) as well as all the assumptions concerning auxiliary non-physical parameters [14] belong to this group of uncertainties.

The global safety formats for NLFEAs proposed by codes [9],[22] and [23]-[24], allow to evaluate the design structural resistance R_d as follows:

$$R_d = \frac{R_{rep}}{\gamma_R \gamma_{Rd}} \tag{1}$$

where

- R_{rep} = representative value of the global structural resistance (i.e., the peak resistance value with reference to cyclic analyses) estimated using NLFEAs;

- γ_R = global resistance partial safety factor which covers the inherent randomness of the material properties;
- γ_{Rd} = resistance model uncertainty partial safety factor that covers all the epistemic uncertainties related to the different assumptions within the model definition.

With specific reference to NLFEAs on RC structural systems under cyclic loads (e.g., the case of earthquake engineering), they may present significantly higher levels of modelling uncertainties if compared to the static loading configurations. In compliance with [14],[25] the resistance model uncertainty random variable ϑ can be expressed as:

$$\vartheta = \frac{R_{Exp}}{R_{NLFEA}} \tag{2}$$

where:

- R_{Exp} = global structural resistance from experimental investigation;
- R_{NLFEA} = global structural resistance from NLFEAs.

3 NLFE MODELLING ASSUMPTIONS AND OUTCOMES FROM NUMERICAL SIMULATIONS

3.1 Characterization and differentiation of the numerical models

As discussed in the previous sections, several modelling hypotheses may be adopted when plane stress NLFEAs are carried out to analyse the seismic response of reinforced concrete structural systems under cyclic loading. Two numerical codes [26]-[27], denoted as numerical code A and B anonymously, are employed to model numerically the experimental tests of [19]-[21] using four-nodes iso-parametric quadrilateral plane stress finite elements having linear interpolant shape functions and 2x2 Gauss integration points. A calibration process of the mesh size has been developed for each experimental test and numerical. The non-linear system of equation is solved by means of the standard Newton-Raphson method [2]. For each load step, the maximum number of iterations has been set equal to 200 adopting the displacement norm convergence criteria with a tolerance set equal to 2%.

A non-linear curve with compression softening and reduction of the compressive strength due to transversal cracking has been used for the concrete behaviour in compression. In detail, the law of [28] is adopted in order to model the mono-axial concrete compressive behaviour both in confined and unconfined zones.

The shear behaviour of concrete has been reproduced associating a constant value to the shear retention factor with the purpose to model the mechanism of aggregate interlock in cyclic response of the shear walls [29]. The un-loading/re-loading process is characterized by a linear relation secant to the origin with reference to both compressive and tensile concrete response [26]-[27]. The uniaxial model for concrete behaviour is extended to plane stress configuration in line with [30]. The smeared cracking with fixed crack direction model has been adopted in order reproduce cracked state concrete [31]. The reinforcement has been modelled by means of a tri-linear constitutive law with cyclic damaging process modelled in compliance to the suggestion of [32]. The reinforcements have been modelled by means of discrete reinforcement with the assumption of perfect bond.

The tensile concrete strength as well as the Young's modulus are derived from the experimental compressive strength in compliance with [33].

An additional discrimination between the modelling hypotheses has been specified with reference to both the concrete tensile response and the shear stiffness of concrete in cracked configuration. As regards the concrete tensile response, the "tension stiffening effect" cannot be neglected. In this way, in addition to the elastic-brittle and to the elastic-plastic model, a third law "LTS (i.e., linear tension softening)" is herein assumed [14]. The first two hypotheses are conceived as lower and upper bounds for tensile response of concrete. The LTS law has been calibrated through an iterative procedure with the aim to best fit each experimental test with the use of a specific numerical code.

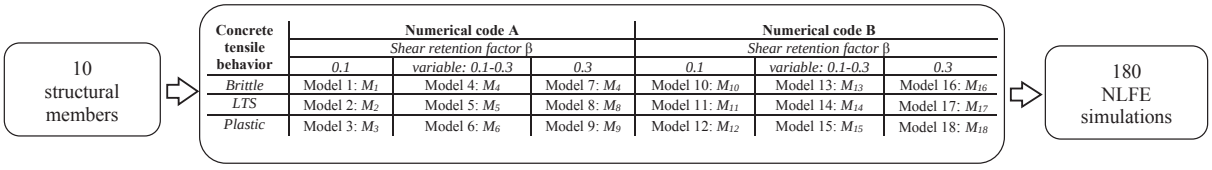

Figure 1: Summary of the 18 modelling hypotheses.

With reference to the shear stiffness, the shear retention factor β, that relates the shear stiffness of concrete after and before cracking, is assumed equal to 0.1 or to 0.3 [34]-[35] or properly calibrated for each numerical code and tensile behaviour and experimental test. In fact, in the third case, an iterative process is used to define the most appropriate value of β within the interval 0.1-0.3 [34]-[35]. Altogether, combining the the three different concrete tensile behaviours with the three different values of shear retention factor and the two numerical codes, 18 different modelling hypotheses (i.e., structural models M_j with $j=1,\ldots,18$ representative of the epistemic uncertainties) derive, as reported in Figure 1.

3.2 Experimental tests and numerical outcomes

The numerical and experimental results of [19]-[21], expressed in terms of lateral load vs displacement diagrams, are herein compared.

The experimental investigation of [19] focus on six reinforced concrete walls designed in pairs in order to have equal percentage of bending reinforcement but different percentage of shear reinforcement. In this study, only 3 walls are taken into consideration denoted respectively as SW4, SW6, SW8. In detail, they have the following geometrical characteristics: 1.20 m high, 0.6 m wide, 0.06 m thick and stiffened by a 0.2 m x 0.25 m inferior beam, and by a 0.2 m x 0.15 m superior beam useful to spread the applied horizontal load. All the walls are subjected to the same load history as showed in Figures 2-4. The tests have been performed in displacement control from 2 mm up to failure, performing two complete cycles with a 2 mm increment each time. The compressive strength of concrete is within the range 36.9 to 45.8 MPa in the different tests, whereas the flexural reinforcement remains constant in the web differently to the shear reinforcement and the vertical reinforcement that vary in the boundary elements. The numerical outcomes from the simulations expressed in terms of peak global structural resistance are presented in Table 1. The outcomes from NLFEAs are reported in Figures 2-4 (a)-(f) with reference to the several modeling hypotheses.

In general, the minimum values of the peak lateral loads are obtained adopting the elastic-brittle constitutive law for concrete tensile behavior, while the numerical models with plastic constitutive law always overestimate both the peak load and stiffness. It can also be observed that the best results are achieved with a shear retention factor equal or close to 0.1 for the tests SW6 and SW8. The simulations generally overestimate the global structural resistance, but underestimate the ductility because many simulations fail before if compared to the experimental results.

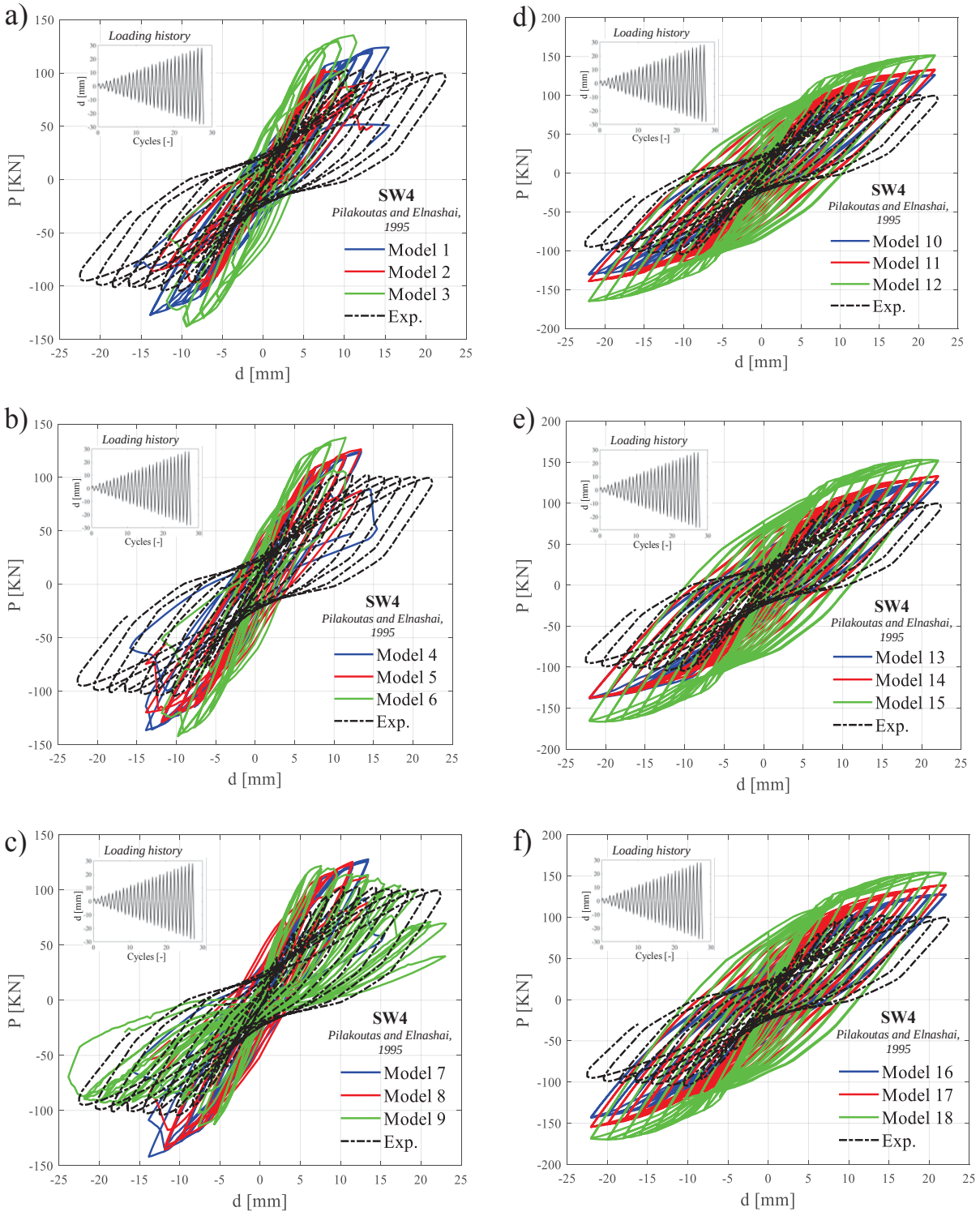

Figure 2: Comparison between NLFEAs and experimental tests expressed as load vs displacement curves - SW4 of [19]; (a-c) Numerical code A, (d-f) Numerical code B.

Figure 2-4 (a-c) and (d-f) show how the dependence of the results on the numerical code choice (numerical code A and B, respectively): in Figure 2-4 (a-c) the numerical models fail before the end of the experimental load history, while in Figure 2-4 (d-f) the simulations reach

the end of the analysis but overestimate the resistance, especially, for the Models 12, 15 and 18. The failure mode consists of the yielding of the main reinforcements and of the crushing of concrete in the boundary compressed element on the opposite side.

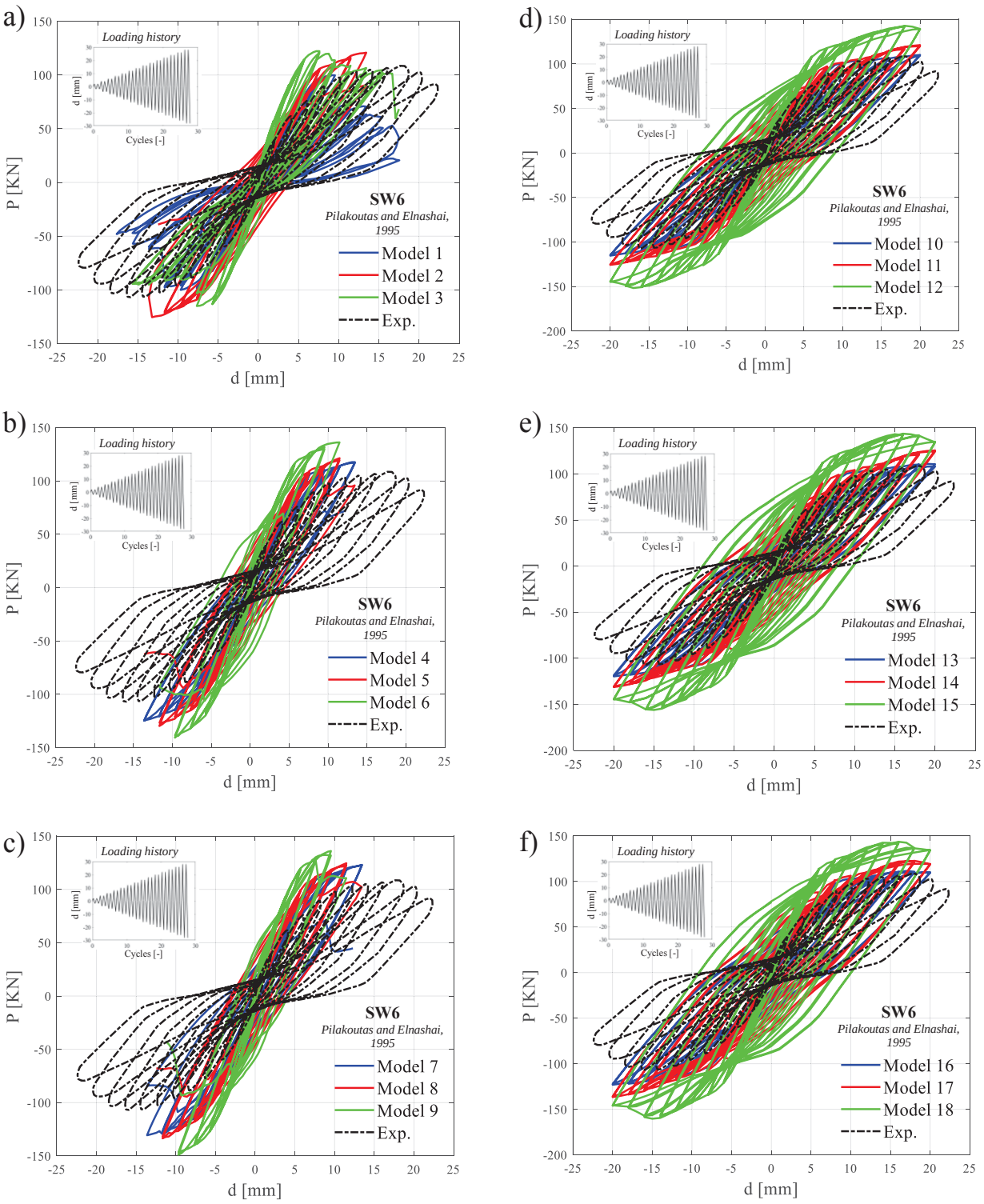

Figure 3: Comparison between NLFEAs and experimental tests expressed as load vs displacement curves – SW6 of [19]; (a-c) Numerical code A, (d-f) Numerical code B.

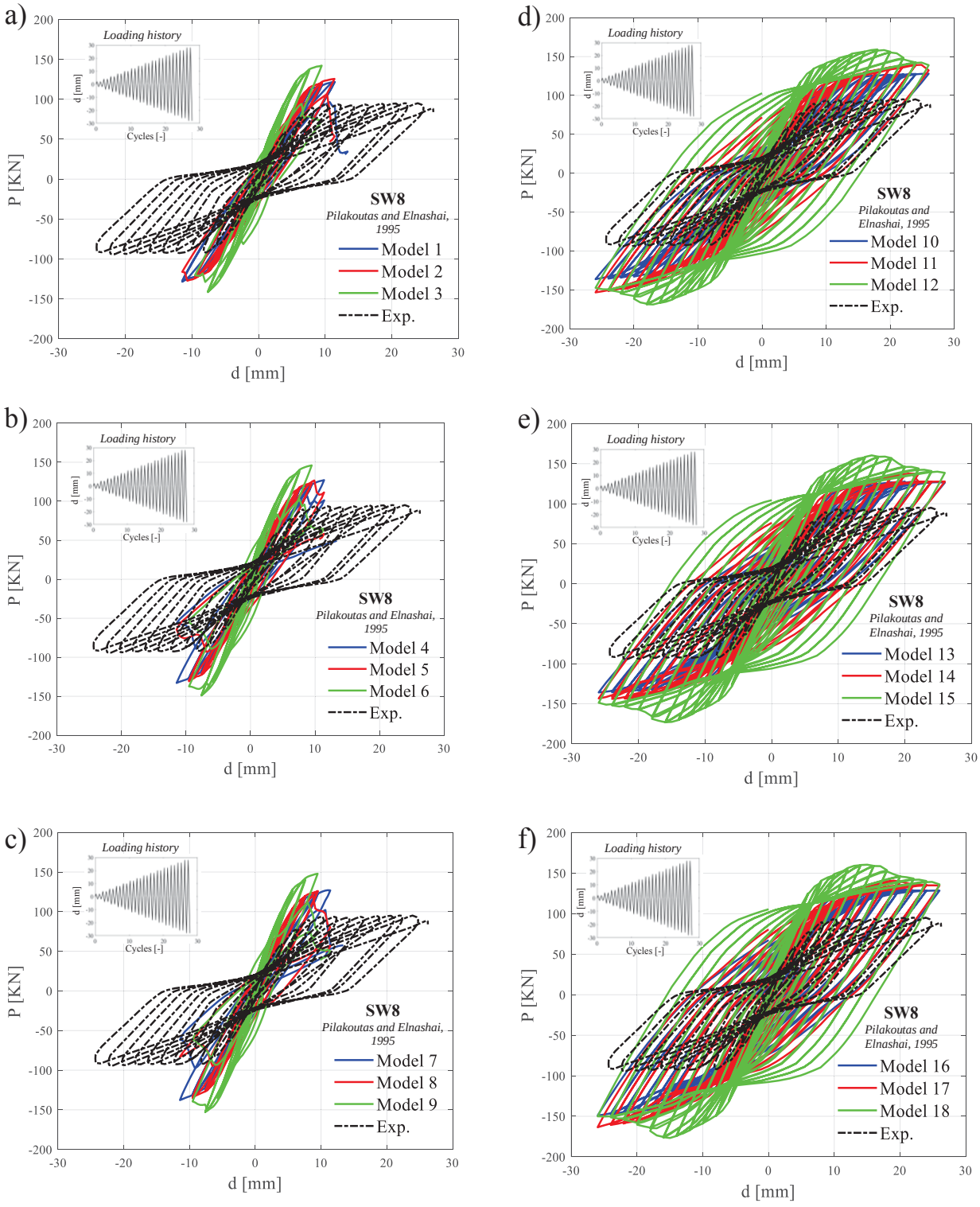

Figure 4: Comparison between NLFEAs and experimental tests expressed as load vs displacement curves – SW8 of [19]; (a-c) Numerical code A, (d-f) Numerical code B.

Exp. Test	R_{Exp}	R_{M1}	R_{M2}	R_{M3}	R_{M4}	R_{M5}	R_{M6}	R_{M7}	R_{M8}	R_{M9}
	kN	kN	kN	kN	kN	kN	kN	kN	kN	kN
SW4	103.0	124.0	103.4	135.4	124.9	126.4	137.4	127.8	125.5	121.8
SW6	108.6	100.1	120.8	122.2	117.6	121.3	134.3	123.0	124.5	136.0
SW8	95.1	128.5	127.3	142.2	133.0	130.9	149.1	137.7	135.2	152.8
Exp. Test	R_{Exp}	R_{M10}	R_{M11}	R_{M12}	R_{M13}	R_{M14}	R_{M15}	R_{M16}	R_{M17}	R_{M18}
	kN	kN	kN	kN	kN	kN	kN	kN	kN	kN
SW4	103.0	126.3	133.5	151.6	125.8	133.1	152.8	127.8	139.1	154.3
SW6	108.6	110.3	121.3	142.9	110.8	125.4	142.7	111.6	122.7	143.7
SW8	95.1	128.0	139.4	159.2	127.8	137.7	160.4	131.9	140.8	160.5

Table 1: Peak resistances from both the experimental tests R_{EXP} [19] and NLFEAs R_{NLFEA} for the different modelling hypotheses.

The experimental tests of [20] concern four identical walls of dimensions 1300x650x65mm, that are constrained inferiorly by a beam of section 200x300mm which simulates a stiff foundation. At the top there is a stiff beam to uniformly transmit the imposed displacement on the top of the wall. The flexural reinforcement is represented by ϕ8/100mm in the web, while the distance is reduced to 70mm in the boundary elements. The shear reinforcement is composed of ϕ6.25/260mm over the entire width of the wall and of additional stirrups of ϕ4/130mm in the boundary elements. The shear walls denoted as SW31, SW32 and SW33 are herein considered for the modelling uncertainty investigation. The experimental tests present a load history composed of four or five cycles with displacements of a few millimeters and then of a monotonic displacement increase up to failure. The compressive strength of concrete varies in the range 35-53 MPa in the different tests. The numerically computed peak global structural resistances are listed in Table 2. Figures 5-7 (a)-(f) show that the models related to elastic-plastic model for the tensile response of concrete (i.e., Models 3, 6, 9, 12, 15, 18) overestimate both the resistance and stiffness, while models having the assumption of elastic-brittle or linear tension softening in tension have more or less the same behavior with a stiffness similar to the actual one in the cyclic phase. In general, an underestimation of the resistance is recognized. It can be also noted that the more the shear retention factor increases (up to the value 0.3), the more the dissipated energy increases too.

Exp. Test	R_{Exp}	R_{M1}	R_{M2}	R_{M3}	R_{M4}	R_{M5}	R_{M6}	R_{M7}	R_{M8}	R_{M9}
	kN	kN	kN	kN	kN	kN	kN	kN	kN	kN
SW31	115.9	111.9	120.8	160.2	121.3	133.3	168.9	127.7	139.3	174.4
SW32	111.0	110.3	114.8	142.8	114.9	118.3	142.7	119.1	131.1	144.3
SW33	111.5	107.2	111.5	129.8	110.4	114.0	139.4	113.8	117.6	143.8
Exp. Test	R_{Exp}	R_{M10}	R_{M11}	R_{M12}	R_{M13}	R_{M14}	R_{M15}	R_{M16}	R_{M17}	R_{M18}
	kN	kN	kN	kN	kN	kN	kN	kN	kN	kN
SW31	115.9	87.8	117.5	139.8	98.0	127.2	147.6	98.9	131.8	151.2
SW32	111.0	93.7	101.6	129.4	93.9	101.9	129.5	99.4	102.2	129.7
SW33	111.5	94.6	96.0	118.7	95.2	101.1	122.8	95.7	98.8	126.9

Table 2: Peak resistances from both the experimental tests R_{EXP} [20] and NLFEAs R_{NLFEA} for the different modelling hypotheses.

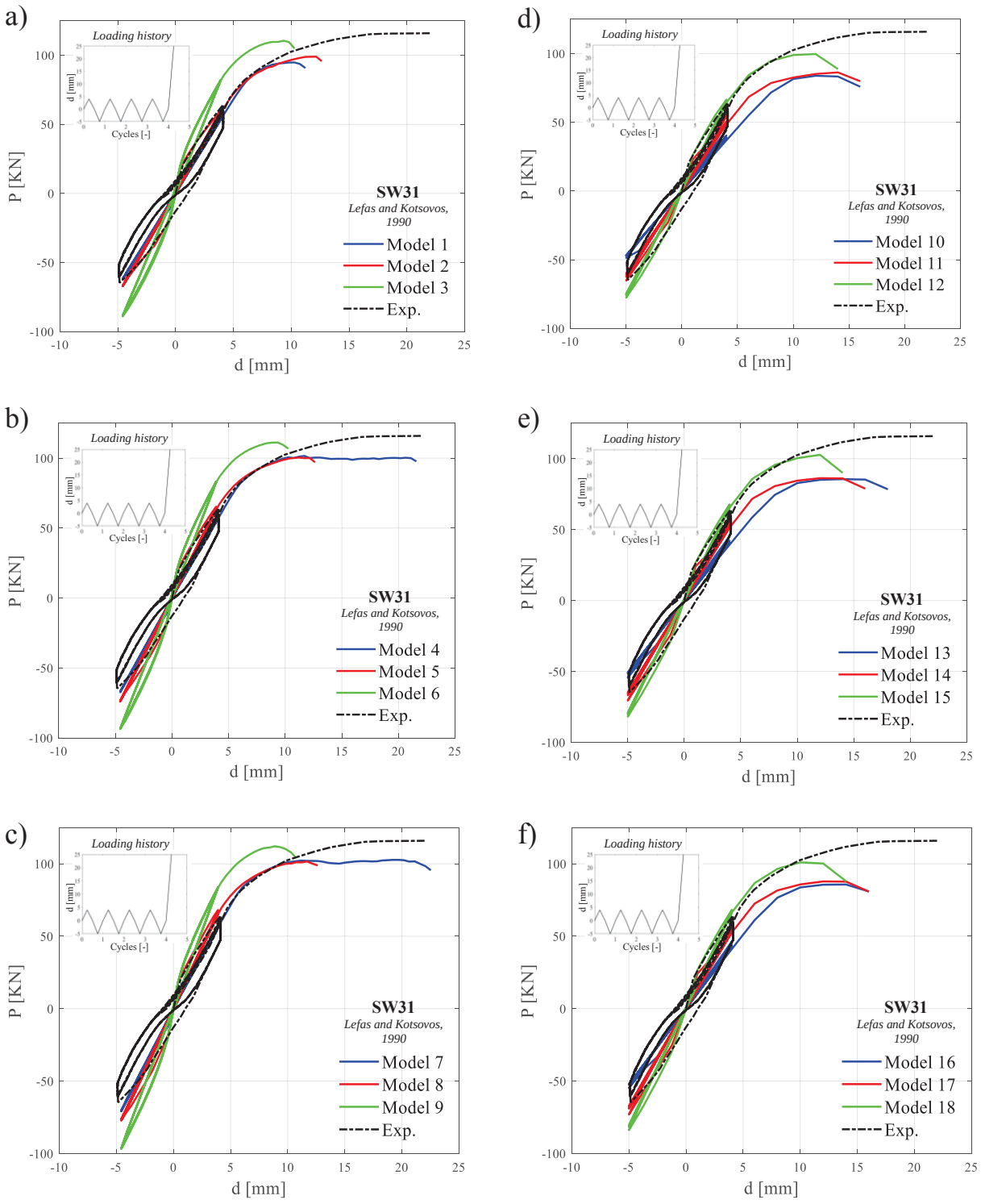

Figure 5: Comparison between NLFEAs and experimental tests expressed as load vs displacement curves – SW31 of [20]; (a-c) Numerical code A, (d-f) Numerical code B.

The failure mode is reached through the yielding of the tensile reinforcements and crushing of concrete located at the bottom of the boundary elements. Some simulations do not reach

the ultimate experimental displacement but fail upon reaching the maximum load or for a slightly greater displacement than the one achieved in the cyclic phase.

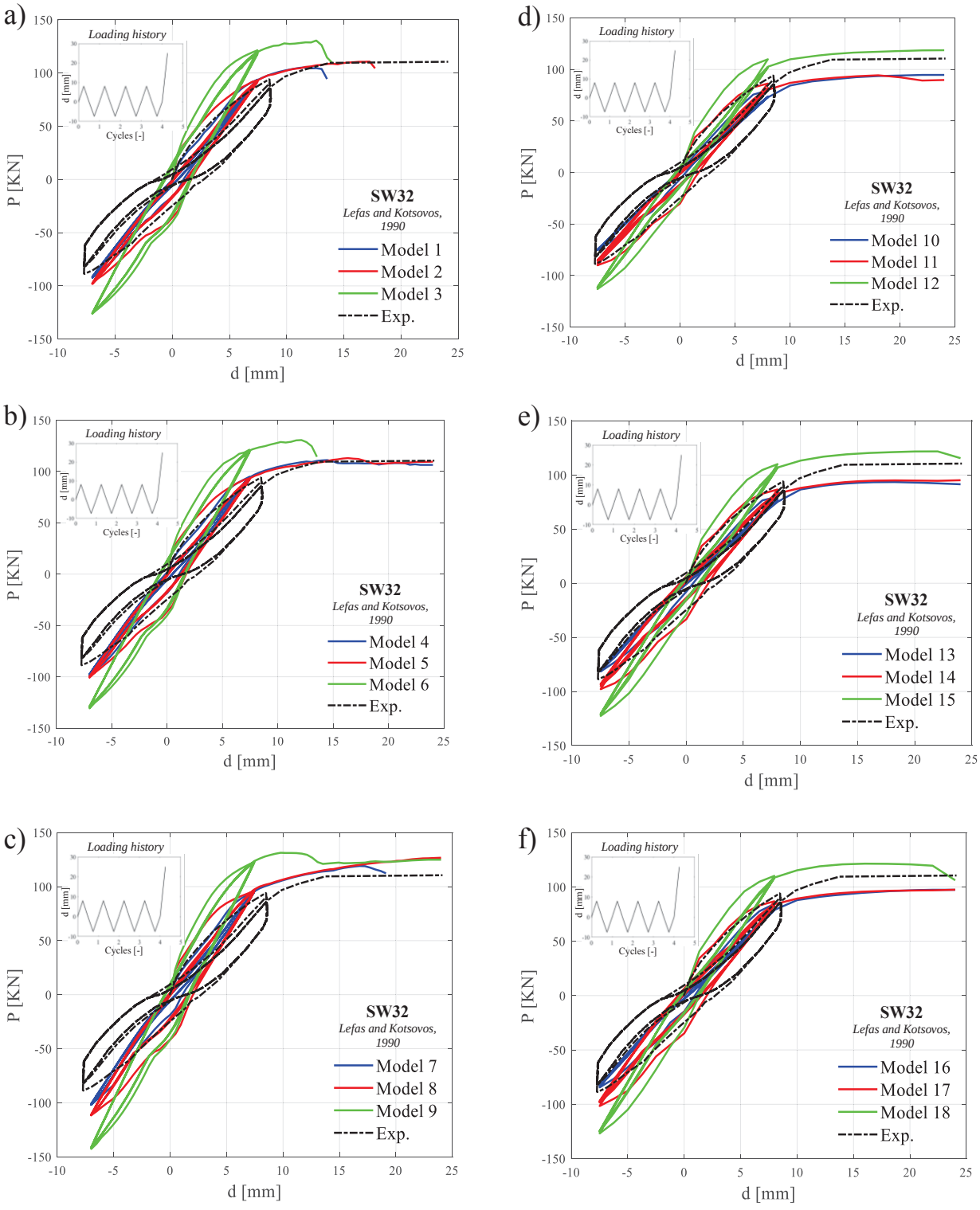

Figure 6: Comparison between NLFEAs and experimental tests expressed as load vs displacement curves – SW32 of [20]; (a-c) Numerical code A, (d-f) Numerical code B.

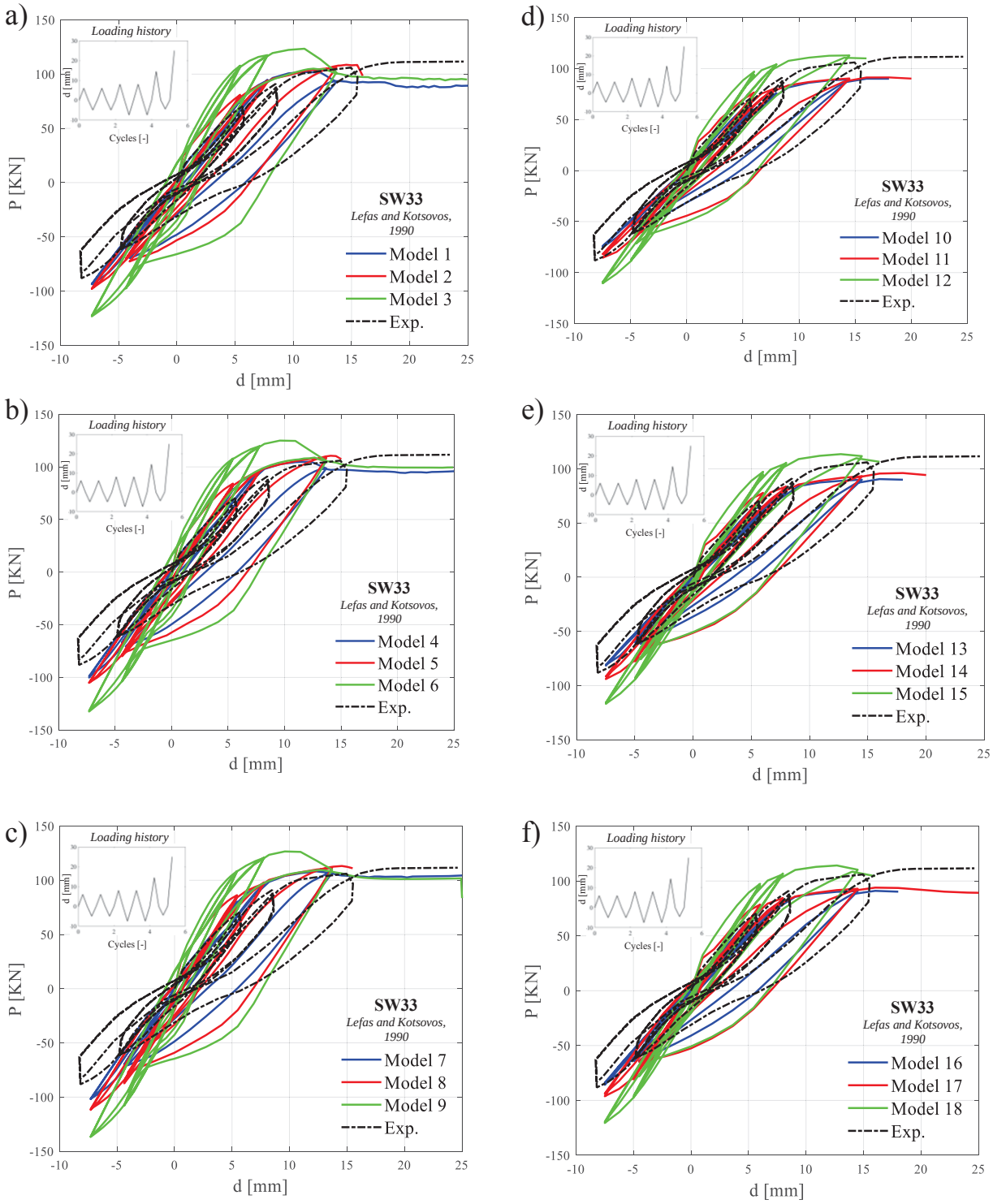

Figure 7: Comparison between NLFEAs and experimental tests expressed as load vs displacement curves – SW33 of [20]; (a-c) Numerical code A, (d-f) Numerical code B.

The laboratory tests of [21] investigate RC walls subjected to a in-plane quasi-static cyclic loading. In detail, four specimens (WSH2, WSH3, WHS4, WSH6) are considered and reproduced by means of numerical simulations. The walls have same geometry (i.e., 4.03 m high, 2 m wide and 0.15 m thick) and are fixed at the base through a beam integral with the support-

ing surface of section 0.6 m high and 0.7 wide and protruding 0.4 m from the two sides of the wall, while at the top there is a 0.4 m thick and 0.92 m high beam with a taper to favourite the connection with the wall. On this beam the axial load is provided and the cyclic loading history is applied by means of actuators located at a distance of 0.39 m from the upper edge. The walls are all reinforced with ϕ6/150 mm located horizontally along the entire width of the wall. They differs in the percentage of flexural reinforcement and in the percentage of shear reinforcement in the boundary element as well as for the value of the applied axial load. The WSH2 wall has flexural reinforcements of 6ϕ10, spaced at 75 mm in the boundary elements, and of 24ϕ6 in the web spaced at 125 mm (symmetrically starting from the outside to the center). The shear reinforcement consists of ϕ6/150 mm across the entire width, as mentioned above, and of stirrups ϕ6/75mm that enclose the ϕ10s and of a ϕ4.2 hoop that binds the two central ϕ10s. The specimen WSH3 is reinforced with 6ϕ12 on the boundary elements spaced at 100 mm, and with 22ϕ8 in the web spaced at 125 mm, and has a shear reinforcement identical to the WSH2. The wall WSH4 differs from the WSH3 concerning the shear reinforcement composed of ϕ6/150 mm across the entire width and of ϕ6/150 mm in the boundary element. The specimenWSH6 has the same bending reinforcement of the previous one with a higher reinforcement percentage in the boundary element. There are ϕ6/50 mm closed stirrups around the four lateral flexural bars, and another closed stirrup of 4.2/50 mm which encloses the four inners ϕ12. The compressive strength of concrete and axial load are similar for WSH2, WSH3 and WSH4 with values of 40.5, 39.2 and 40.9 MPa and 691, 686 and 695 kN, respectively. While WSH6 has a higher compressive strength equal to 45.6 MPa and an axial load of 1476 kN. The loading history is in line with the standard protocol by [36].

Exp. Test	R_{Exp}	R_{M1}	R_{M2}	R_{M3}	R_{M4}	R_{M5}	R_{M6}	R_{M7}	R_{M8}	R_{M9}
	kN	kN	kN	kN	kN	kN	kN	kN	kN	kN
WSH2	359.0	378.3	363.2	512.0	386.0	369.4	521.6	436.6	407.5	562.5
WSH3	454.0	441.4	443.6	604.8	454.0	448.9	659.5	549.1	474.3	674.2
WHS4	443.0	450.8	448.9	508.5	467.6	450.7	525.9	484.2	523.8	567.7
WSH6	597.0	633.9	624.4	732.7	665.2	658.3	744.8	689.0	678.2	794.9
Exp. Test	R_{Exp}	R_{M10}	R_{M11}	R_{M12}	R_{M13}	R_{M14}	R_{M15}	R_{M16}	R_{M17}	R_{M18}
	kN	kN	kN	kN	kN	kN	kN	kN	kN	kN
WSH2	359.0	376.9	410.1	493.8	367.7	413.7	489.9	389.6	410.3	488.6
WSH3	454.0	481.6	532.7	603.6	500.1	542.2	617.0	483.1	532.4	607.3
WHS4	443.0	404.8	441.5	474.4	423.3	442.1	481.0	435.5	457.8	483.5
WSH6	597.0	617.7	661.6	739.5	624.8	664.4	758.2	638.6	673.4	768.9

Table 3: Peak resistances from both the experimental tests R_{EXP} [21] and NLFEAs R_{NLFEA} for the different modelling hypotheses.

At each displacement level the wall has been subjected to two full cycles. The results of numerical simulations expressed as peak global structural resistance are presented in Table 3. Figures 8-11 (a)-(f) show that assuming the tensile behaviour of the concrete brittle or LTS reproduces efficiently the actual behaviour, while the models with concrete tensile behaviour perfectly plastic overestimate both the resistance and stiffness.

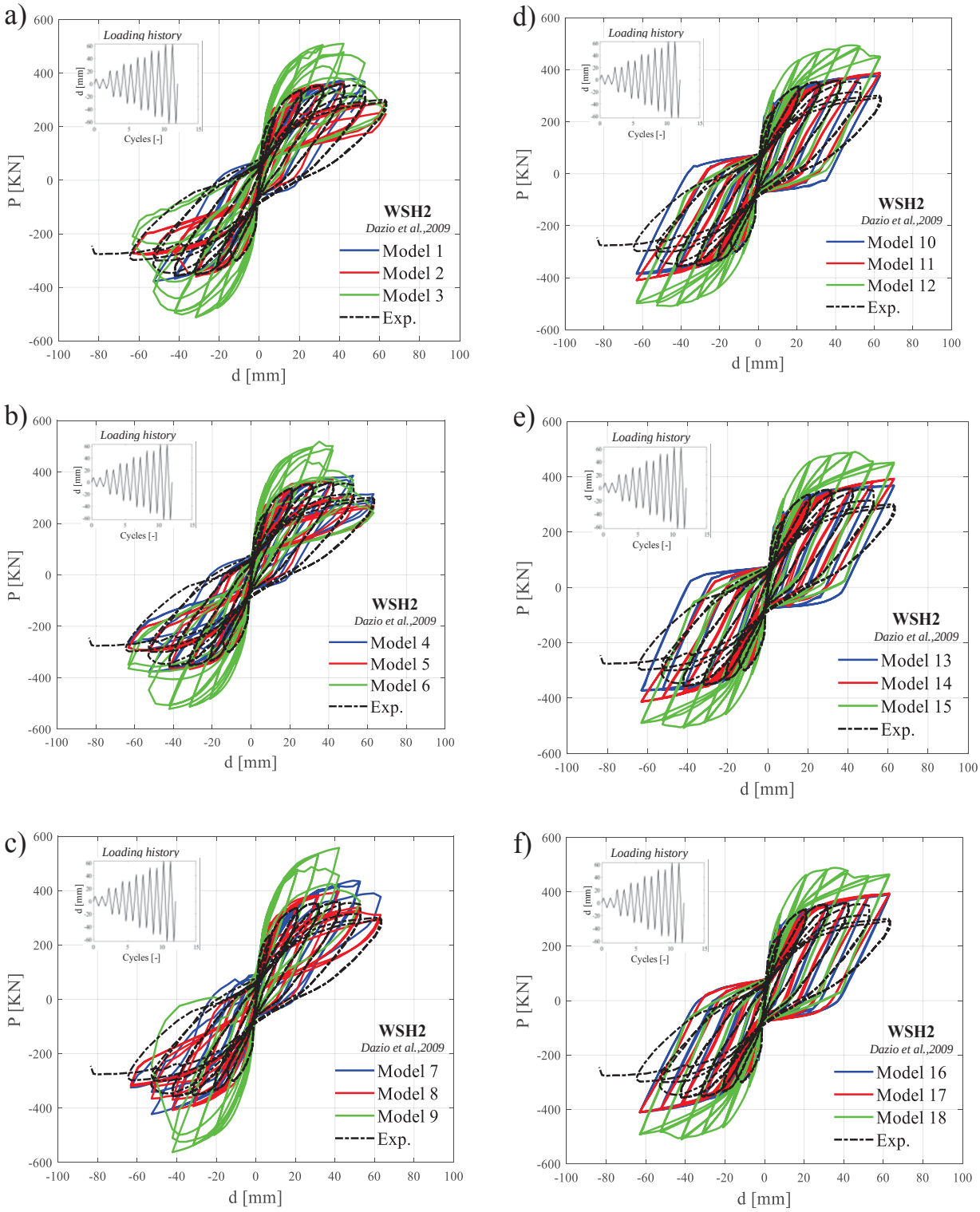

Figure 8: Comparison between NLFEAs and experimental tests expressed as load vs displacement curves – WSH2 of [21]; (a-c) Numerical code A, (d-f) Numerical code B.

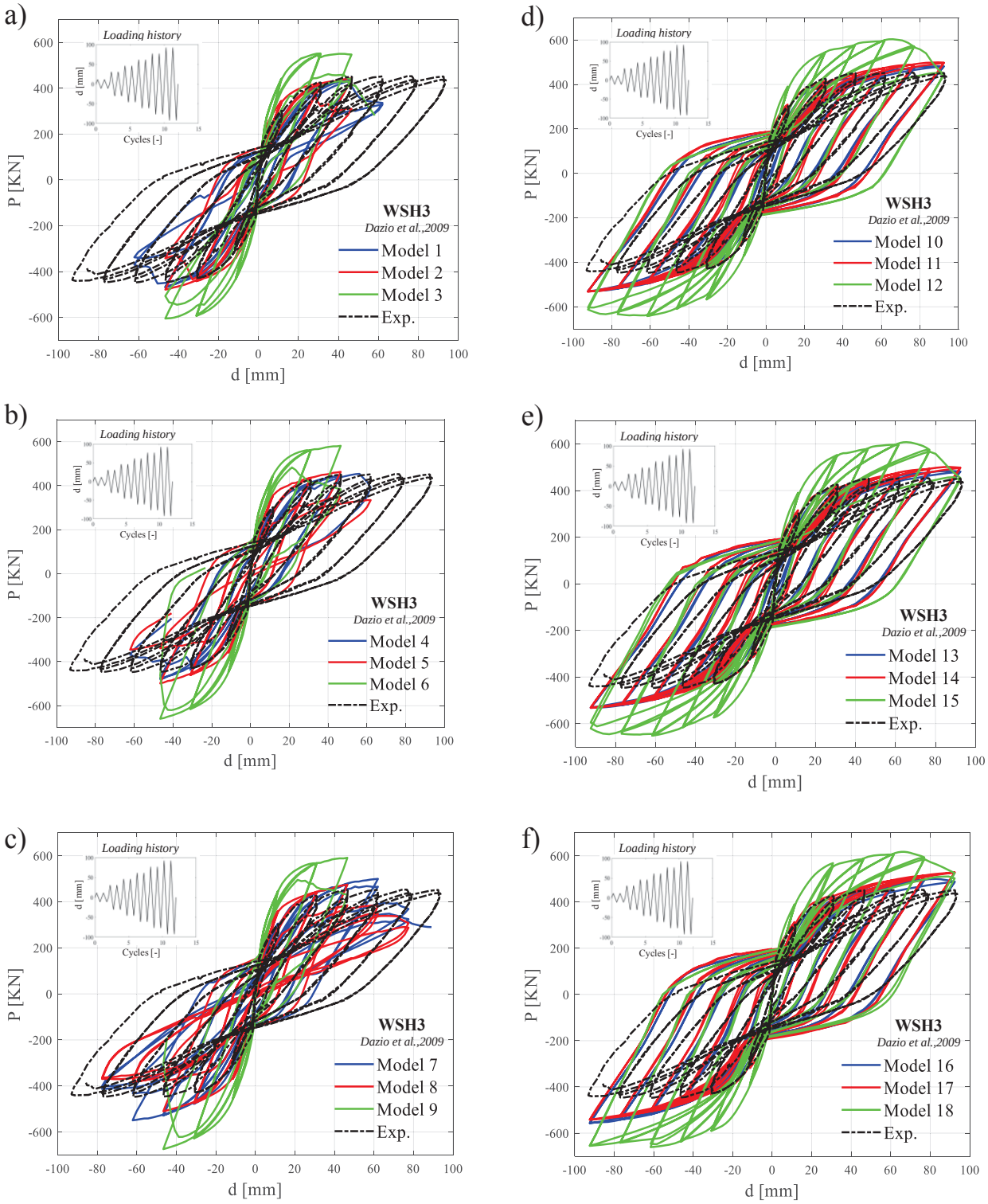

Figure 9: Comparison between NLFEAs and experimental tests expressed as load vs displacement curves – WSH3 of [21]; (a-c) Numerical code A, (d-f) Numerical code B.

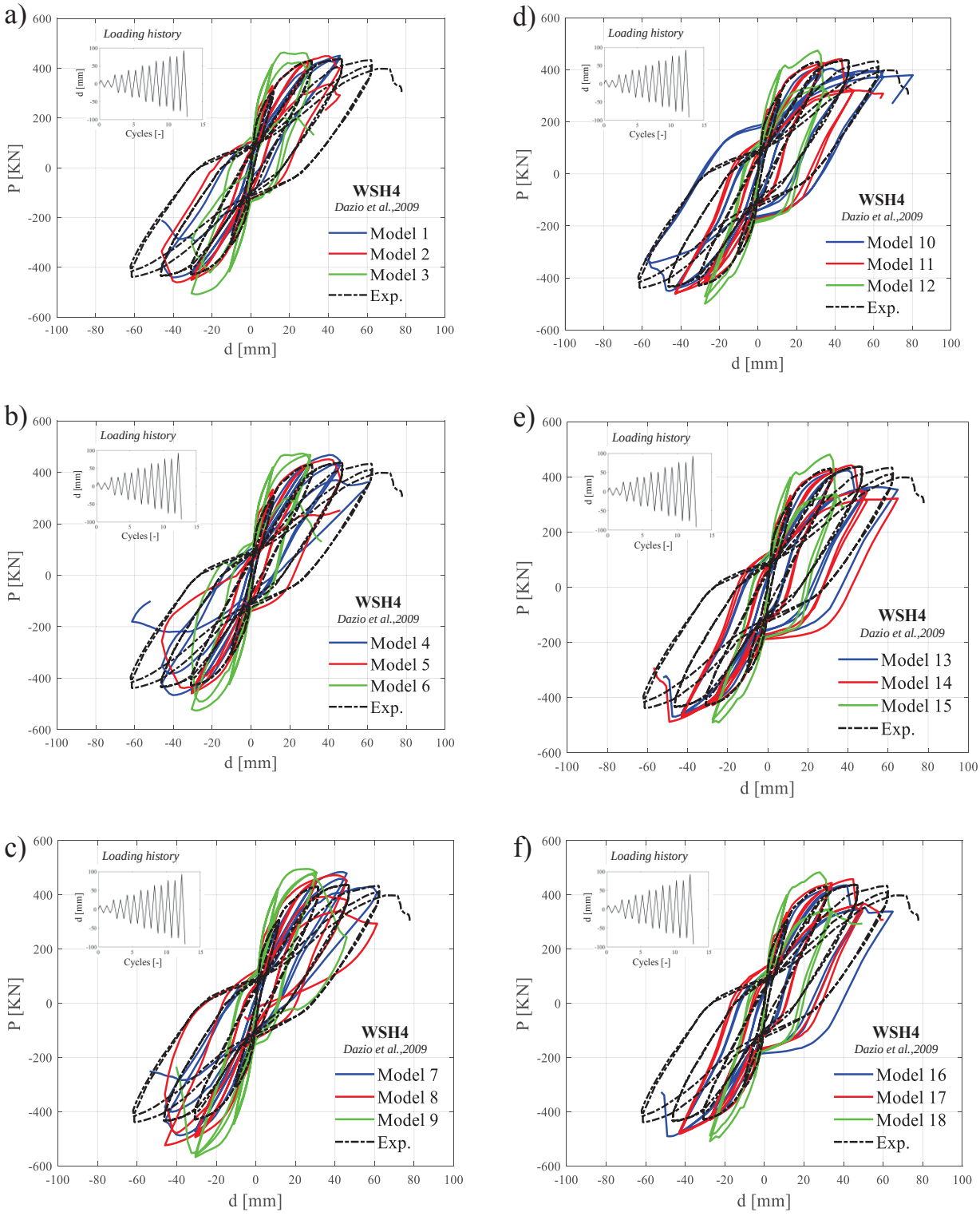

Figure 10: Comparison between NLFEAs and experimental tests expressed as load vs displacement curves – WSH4 of [21]; (a-c) Numerical code A, (d-f) Numerical code B.

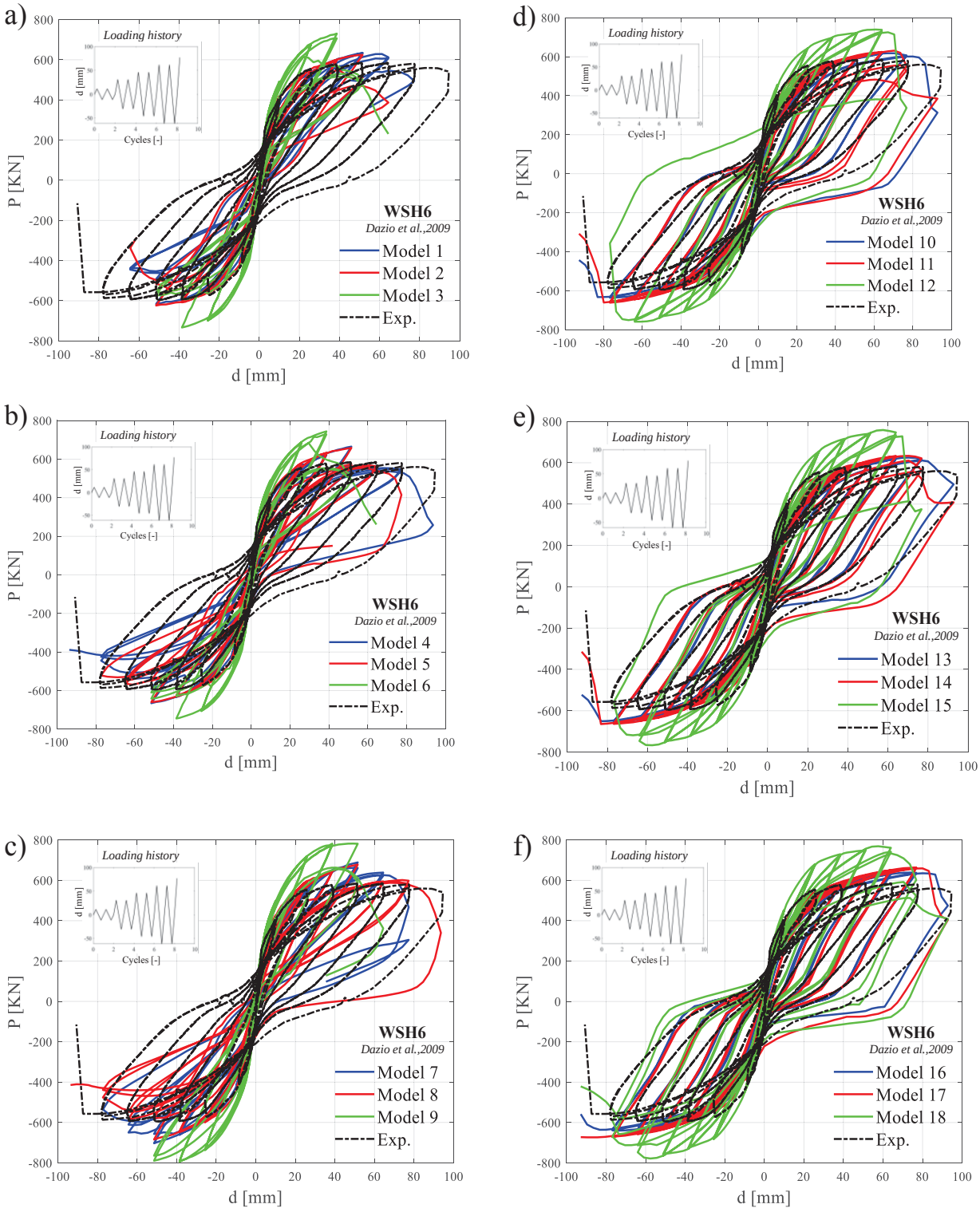

Figure 11: Comparison between NLFEAs and experimental tests expressed as load vs displacement curves – WSH6 of [21]; (a-c) Numerical code A, (d-f) Numerical code B.

4 DISCUSSION

The results deriving from the abovementioned 180 non-linear FE simulations can be used in order to quantify the resistance model uncertainties in plane stress NLFEAs of RC structures under cyclic loads. These results show the several difficulties in reproducing the actual failure behaviour of structural members. The outcomes in terms of ratio $\vartheta = R_{Exp}/R_{NLFEA}$ reported in Table 4 demonstrate that the two extreme hypotheses regarding concrete tensile behaviour (i.e., elastic-brittle and elastic-plastic) do not represent in all the cases the bound limits concerning the experimental peak of resistance.

Exp. Test	M_1	M_2	M_3	M_4	M_5	M_6	M_7	M_8	M_9
	-	-	-	-	-	-	-	-	-
SW4	0.83	1.00	0.76	0.82	0.81	0.75	0.81	0.82	0.85
SW6	1.08	0.90	0.89	0.92	0.90	0.81	0.88	0.87	0.80
SW8	0.74	0.75	0.67	0.72	0.73	0.64	0.69	0.70	0.62
SW31	1.04	0.96	0.72	0.96	0.87	0.69	0.91	0.83	0.66
SW32	1.01	0.97	0.78	0.97	0.94	0.78	0.93	0.85	0.77
SW33	1.04	1.00	0.86	1.01	0.98	0.80	0.98	0.95	0.78
WSH2	0.95	0.99	0.70	0.93	0.97	0.69	0.82	0.88	0.64
WSH3	1.03	1.02	0.75	1.00	1.01	0.69	0.83	0.96	0.67
WHS4	0.98	0.99	0.87	0.95	0.98	0.84	0.91	0.85	0.78
WSH6	0.94	0.96	0.81	0.90	0.91	0.80	0.87	0.88	0.75
Mean	0.96	0.95	0.78	0.92	0.91	0.75	0.86	0.86	0.73
CoV	10%	8%	9%	9%	9%	8%	9%	8%	10%

Exp. Test	M_{10}	M_{11}	M_{12}	M_{13}	M_{14}	M_{15}	M_{16}	M_{17}	M_{18}
	-	-	-	-	-	-	-	-	-
SW4	0.82	0.77	0.68	0.82	0.77	0.67	0.81	0.74	0.67
SW6	0.98	0.90	0.76	0.98	0.87	0.76	0.97	0.88	0.76
SW8	0.74	0.68	0.60	0.74	0.69	0.59	0.72	0.68	0.59
SW31	1.32	0.99	0.83	1.18	0.91	0.79	1.17	0.88	0.77
SW32	1.18	1.09	0.86	1.18	1.09	0.86	1.12	1.09	0.86
SW33	1.18	1.16	0.94	1.17	1.10	0.91	1.16	1.13	0.88
WSH2	0.95	0.88	0.73	0.98	0.87	0.73	0.92	0.87	0.73
WSH3	0.94	0.85	0.75	0.91	0.84	0.74	0.94	0.85	0.75
WHS4	1.09	1.00	0.93	1.05	1.00	0.92	1.02	0.97	0.92
WSH6	0.97	0.90	0.81	0.96	0.90	0.79	0.93	0.89	0.78
Mean	1.02	0.92	0.79	1.00	0.90	0.78	0.98	0.90	0.77
CoV	16%	15%	13%	14%	14%	13%	14%	15%	12%

Table 4: $\vartheta = R_{Exp}/R_{NLFEA}$ for all the modelling hypotheses and related mean values and coefficient of variations (CoV).

These results highlight the effectiveness of the different assumptions to reproduce the cyclic response of the structural members. In fact, the differences between the experimental and the numerically predicted resistances may be significantly high: unsafe values up to 0.64 are obtained for the shear walls SW8 and WSH2. It means that the finite element models are not always able to reproduce the experimental behaviour accurately but sometimes overestimate the peak resistances of the walls under specific hypotheses leading to unsafe estimations. This issue is a crucial aspect in relation to safety verifications for seismic analyses. With reference

to each numerical model M_j, Table 4 also reports the mean value and coefficient of variation (CoV). The lowest unsafe bias is achieved for model M_6 and M_9 as well as concerning models M_{10} to M_{18} the highest dispersion are recognised. In particular, a substantial difference can be noted between Numerical code A and B. In fact, the numerical code A seems to provide slightly unsafe bias factors with respect to the numerical code B (in average, 0.85 against 0.90, respectively). Concerning the coefficient of variation, the numerical code A presents a lower level of dispersion of the data with respect to the numerical code B (in average, 9% against 14%, respectively). These results can be useful to develop statistical and probabilistic analyses [37]-[42] to interpret and treat the model uncertainty variable θ. Moreover, it is also highlighted that the choice of the type of software to solve a specific structural problem is relevant. More details may be found in [43].

5 CONCLUSIONS

The present investigation is devoted to quantify the resistance model uncertainties when the global structural resistance of RC structural systems under cyclic loads is estimated through plane non-linear finite element method analyses. A set of experimental tests concerning different walls subject of cyclic shear actions have been numerically simulated by means of 180 NLFEAs combining two different numerical codes, three different constitutive laws for the tension behaviour of concrete and three different shear retention factors. It can be observed that when the tensile behaviour for concrete is assumed perfectly plastic, a greater overestimation of the structural resistance always derives as well as the shear retention factor varies the amplitude of the cycle, and therefore influences the dissipated energy. However, in terms of resistance, a shear retention factor assumed close to 0.1 is the one that allows to obtain the best results with respect to the experimental outcomes. The average bias factor between the different modelling hypotheses is quantified as 0.88 with an average coefficient of variation of 11%.

ACKNOWLEDGEMENTS

This work is part of the collaborative activity developed by the authors within the framework of the Commission 3 – Task Group 3.1: "Reliability and safety evaluation: full-probabilistic and semi-probabilistic methods for existing structures" of the International Federation for Structural Concrete (*fib*).

This work is also part of the collaborative activity developed by the authors within the framework of the WP 11 – Task 11.4 – ReLUIS.

REFERENCES

[1] B. Belletti, C. Damoni, MAN Hendriks, Development of guidelines for nonlinear finite element analyses of existing reinforced and prestressed beams. *European Journal of Environmental and Civil Engineering*, 15(9): 1361-1384, 2011.

[2] *fib* Bulletin N°45, Practitioner's guide to finite element modelling of reinforced concrete structures – State of the art report. Lausanne, 2008.

[3] Troisi R., Alfano G. 2019. Towns as Safety Organizational Fields: An Institutional Framework in Times of Emergency. *Sustainability*, 11: 7025, 2019, doi:10.3390/su11247025.

[4] Troisi R., Alfano G. 2020. Firms'crimes and land use in Italy. An exploratory data anlysis. New Metropolitan Perspectives, International Symposium – 4th edition, 27-30 May 2020, pp 10.

[5] D. La Mazza, L. Giordano, P. Castaldo, D. Gino, Assessment of the efficiency of seismic design for structural robustness of rc structures , *Ingegneria Sismica*, 34(3-4): 63-77, 2017.

[6] D. Gino, G. Bertagnoli, G. Mancini, Effect of endogenous deformations on composite bridges. Recent Progress in Steel and Composite Structures - *Proceedings of the 13th International Conference on Metal Structures, ICMS 2016*, 15-17 June 2016, Zielona Gora, Poland, pp. 287-298, 2016.

[7] DL. Allaix, VI. Carbone, G. Mancini G. Global safety format for non-linear analysis of reinforced concrete structures. *Structural Concrete,*14(1): 29-42, 2013.

[8] H. Shlune, K. Gylltoft, M. Plos, Safety format for non-linear analysis of concrete structures. *Magazine of Concrete Research,* 64(7): 563-574, 2012.

[9] CEN EN 1992-2 Eurocode 2 Design of concrete structures, Part 2: concrete bridges. *CEN 2005*. Brussels.

[10] *fib* Model Code for Concrete Structures 2010. Lausanne. 2013.

[11] P. Castaldo, D. Gino, G. Mancini, Safety formats for non-linear analysis of reinforced concrete structures: discussion, comparison and proposals. *Engineering Structures*, 193,136-153, 2019.

[12] M. Blomfors, M. Engen, M. Plos, Evaluation of safety formats for non-linear finite element analyses of statically indeterminate concrete structures subjected to different load paths. *Structural Concrete*, 17(1): 44-51, 2016.

[13] V. Cervenka, Reliability-based non-linear analysis according to fib Model Code 2010. *Structural Concrete*. 14(1): 19-28, 2013.

[14] P. Castaldo, D. Gino, G. Bertagnoli, G. Mancini, Partial safety factor for resistance model uncertainties in 2D non-linear finite element analysis of reinforced concrete structures. *Engineering Structures,* 176:746-762, 2018.

[15] P. Castaldo, D. Gino, VI. Carbone, G. Mancini, Framework for definition of design formulations from empirical and semi-empirical resistance models, *Structural Concrete*, 19(4): 980-987, 2018.

[16] D. Gino, P. Castaldo, G. Bertagnoli, L. Giordano, G. Mancini, Partial factor methods for existing structures according to *fib* Bulletin 80: Assessment of an existing prestressed concrete bridge. *Structural Concrete*, 31: 15-31, 2020. https://doi.org/10.1002/suco.201900231

[17] Castaldo P., Alfano G. Seismic reliability-based design of hardening and softening structures isolated by double concave sliding devices, *Soil Dynamics and Earthquake Engineering*, 129: 105930, 2020.

[18] AD. Kiureghian, O. Ditlevsen, Aleatory or epistemic? Does it matter?,M *Structural Safety,* 31: 105-112, 2009.

[19] K. Pilakoutas, A. Einashai, Cyclic Behaviour of Reinforced Concrete Cantilever Walls, Part I : Experimental Results, *ACI Structural Journal*, no.92-S25, 1995.

[20] ID. Lefas, MD. Kotsovos, Strength and deformation characteristics of reinforced concrete walls under load reversals. *ACI Structural Journal,* no.87-S74, 1990.

[21] A. Dazio, K. Beyer, H. Bachmann, Quasi-static cyclic tests and plastic hinge analysis of RC structural walls. *Engineering Structures* 31: 1556-1571, 2009.

[22] *fib* Model Code for Concrete Structures 2010. 2013. Lausanne.

[23] M. Blomfors, M. Engen, M. Plos, Evaluation of safety formats for non-linear finite element analyses of statically indeterminate concrete structures subjected to different load paths. *Structural Concrete*, 17(1): 44-51, 2016.

[24] V. Cervenka, Reliability-based non-linear analysis according to fib Model Code 2010. *Structural Concrete*. 14(1): 19-28, 2013.

[25] M. Holický, J.V. Retief, M. Sikora, Assessment of model uncertainties for structural resistance. *Probabilistic Engineering Mechanics.* 45: 188-197, 2016.

[26] ATENA 2D v5. 2014. *Cervenka Consulting s.r.o*. Prague. Czech Republic.

[27] DIANA FEA BV 2018. Delftechpark 19a 2628 XJ Delft. The Netherlands.

[28] M. Saatcioglu, S.R. Razvi, Strength and ductility of confined concrete. *Journal of Structural engineering,* 118(6):1590–1607, 1992.

[29] B. Belletti, M. Scolari, F. Vecchi, PARC_CL 2.0 crack model for NLFEA of reinforced concrete structures under cyclic loadings. *Computer and Structures,* 191: 165-179, 2017.

[30] H.B. Kupfer, H.K. Gerstle, Behavior of Concrete under Biaxial Stresses. *Journal Engineering Mechanics Division,* 99(4), 1973.

[31] H.R. Riggs, G.H. Powell, Rough crack model for analysis of concrete. *J. Eng. Mech. Div. ASCE*, 112(5): 448-464, 1986.

[32] M. Menegotto, E. Pinto, Method of analysis for cyclically loaded reinforced concrete plane frames including changes in geometry and non-elastic behavior of elements under combined normal force and bending, *Proceedings, IABSE Symposium*. Lisbon, Portugal, 1973.

[33] EN 1992-1-1. Eurocode 2 – Design of concrete structures. Part 1-1: general rules and rules for buildings. CEN 2014. Brussels.

[34] D.L. Araújo, L.C. Carmo, F.G.T. Nunes, R.D.T. Filho, Computational modelling of steel fibre reinforced Concrete beams subjected to shear. *IBRACON Structures and Materials Journal*, vol. 3, n1, 2010.

[35] E. Fehiling, T. Bullo, Ultimate load capacity of reinforcement steel fibre concrete deep beams subjected to shear. *Finite elements in Civil Engineering Applications*, Hendriks & Rots, 2002.

[36] R. Park, Ductility evaluation from laboratory and analytical testing. In: *Proceedings of the 9th world conference on earthquake engineering*. Vol. III, 1988.

[37] Garzillo C., Troisi R. Le decisioni dell'EMA nel campo delle medicine umane. In EMA e le relazioni con le Big Pharma - I profili organizzativi della filiera del farmaco, G. Giappichelli, 85-133, 2015.

[38] Golzio L. E., Troisi R. The value of interdisciplinary research: a model of interdisciplinarity between legal re-search and research in organizations. *Journal For Development And Leadership*, 2: 23-38, 2013.

[39] Nese A.; Troisi R. Corruption among mayors: evidence from Italian Court of Cassation judgments, *Trends In Organized Crime*, 1-26, 2018. DOI:10.1007/s12117-018-9349-4.

[40] Troisi R., Golzio, L. E. Legal studies and organization theory: a possible cooperation. *Manageable cooperation* - European Academy of Management: 16th EURAM Conference, Paris, 1-2, 1-4 June 2016.

[41] Troisi R., Guida V. Is the Appointee Procedure a Real Selection or a Mere Political Exchange? The Case of the Italian Health-Care Chief Executive Officers. *Journal of Entrepreneurial and Organizational Diversity*, 7 (2): 19-38, 2018, DOI:10.5947/jeod.2018.008.

[42] Troisi R. Le risorse umane nelle BCC: lavoro e motivazioni al lavoro. In Progetto aree bianche. Il sistema del credito cooperativo in Campania, 1: 399-417, 2012.

[43] Castaldo, P., Gino, D., Bertagnoli, G. & Mancini, G. Resistance model uncertainty in non-linear finite ele-ment analyses of cyclically loaded reinforced concrete systems, *Engineering Structures*, 211: 110496, 2020, https://doi.org/10.1016/j.engstruct.2020.110496.